EARTH'S CRYOSPHERE
SCIENTIFIC JOURNAL

Earth`s Cryosphere, 2019, vol. XXIII, No. 1, pp. 54–61 **http://earthcryosphere.ru/**

PERMAFROST ENGINEERING

DOI: 10.21782/EC2541-9994-2019-1(54-61)

OPERATION OF THERMOSYPHONS BENEATH AN OIL TANK AT THE VARANDEY FIELD: PREDICTION BY STOCHASTIC ANALYSIS

V.P. Melnikov[1–3], G.V. Anikin[3], K.A. Spasennikova[3]

[1]*Tyumen State University, 6, Volodarskogo str., Tyumen, 625003, Russia; melnikov@ikz.ru*
[2]*Tyumen Industrial University, 38, Volodarskogo str., Tyumen, 625000, Russia*
[3]*Earth Cryosphere Institute, Tyumen Scientific Centre SB RAS, 86, Malygina str., Tyumen, 625000, Russia; anikin@ikz.ru, kspasennikova@gmail.com*

The results of 3D simulation are compared, for the first time, with logged ground temperatures in permafrost which is stabilized by low-angle inclined thermosyphons beneath a hot oil tank at the Varandey oil field. Temperature variations beneath the oil tank are predicted by stochastic analysis using the calculated heat loss from the finned surface of thermosyphons. The estimated probability of finding unfrozen soil in presumably frozen areas in the vicinities of two logged boreholes parallel and perpendicular to the tank bottom is about ~4 %. The predicted temperature distribution agrees well with the measured data.

Temperature field, permafrost, thermosyphon, stochastic prediction, Stefan problem

INTRODUCTION

Permafrost beneath buildings and structures is commonly stabilized with refrigeration systems based on natural convection (two-phase thermosyphons). The operation and performance of thermosyphons have to be simulated appropriately to ensure the designed stability.

We suggested a software [*Anikin and Spasennikova, 2013; Plotnikov et al., 2017*] which was advantageous over other existing codes as it could predict the state of soil with regard to climate variability and estimate the probability for frozen/unfrozen soil to occur at an arbitrary point of the modeling domain.

The workability of the software has been checked by comparing the results of 3D simulation and temperature logging of thermally stabilized ground under an oil tank (a vertical steel tank VST-1.4) at the Varandey oil field [*Anikin et al., 2011b*].

The temperature distribution under an oil tank can be predicted by the stochastic analysis using heat loss data [*Anikin et al., 2017a,b*]. The calculation methods were detailed in previous publications [*Anikin et al., 2011a, 2013; Anikin and Spasennikova, 2012; Dolgikh et al., 2013, 2014, 2015; Melnikov et al., 2014*].

PROBLEM FORMULATION

The thermal stabilization system (Fig. 1) beneath the oil tank at the Varandey field was launched in April 2006. The oil tank, which stores oil at 45 °C, has inner and outer walls (inner and outer diameters d_{in} = 60.7 m and d_{out} = 66.07 m, respectively), with air

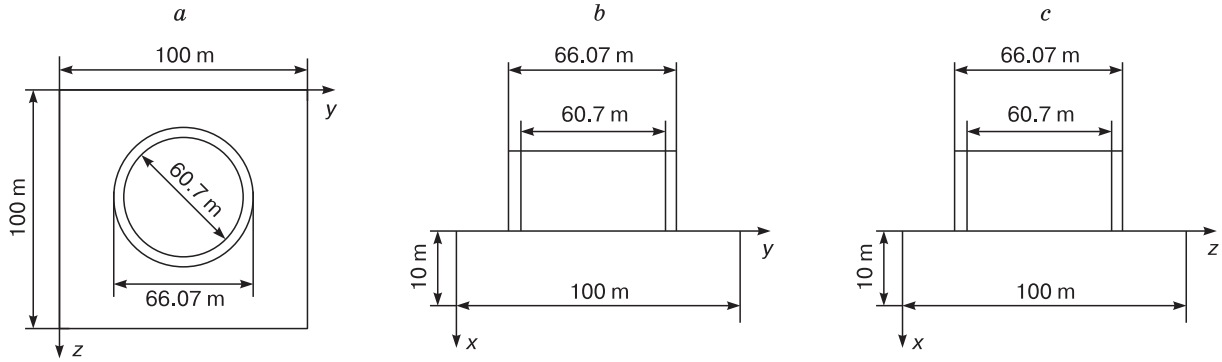

Fig. 1. Geometry of modeling domain in three coordinate planes:

a: (*y*, *z*); *b*: (*x*, *y*); *c*: (*x*, *z*).

between them to prevent lateral heat flux. The tank stands on a hydrophobic layer which, in its turn, lies over a layer of thermal insulator. The thicknesses and thermal conductivities of the two layers are, respectively, l_1 = 0.6 m and λ_1 = 0.95 W/(m·°C); l_2 = 0.4 m and λ_2 = 0.041 W/(m·°C).

The field of ground temperatures is calculated using the following derivation [*Anikin et al., 2009, 2013; Anikin and Spasennikova, 2012; Dolgikh et al., 2013, 2014*]:

$$t(i,j,k,n+1) = t(i,j,k,n) +$$

$$+\frac{a(i,j,k)h_\tau\left(t(i+1,j,k,n)+t(i-1,j,k,n)-2t(i,j,k,n)\right)}{h_x^2}+$$

$$+\frac{a(i,j,k)h_\tau\left(t(i,j+1,k,n)+t(i,j-1,k,n)-2t(i,j,k,n)\right)}{h_y^2}+$$

$$+\frac{a(i,j,k)h_\tau\left(t(i,j,k+1,n)+t(i,j,k-1,n)-2t(i,j,k,n)\right)}{h_z^2},$$

where $t(i, j, k, n)$ is the ground temperature at the point with the coordinates x_i, y_j and z_k at the time τ_n.

The space and time coordinates in the modeling domain are specified as

$$x_i = ih_x, \quad 0 \leqslant i \leqslant 101, \quad h_x = 0.1 \text{ m},$$

$$y_j = jh_y, \quad 0 \leqslant j \leqslant 1001, \quad h_y = 0.1 \text{ m},$$

$$z_k = kh_z, \quad 0 \leqslant k \leqslant 101, \quad h_z = 1 \text{ m},$$

$$\tau_n = h_\tau n, \quad h_\tau = 0.01 \text{ day},$$

where h_x, h_y and h_z are the space stepsizes along the x, y and z axes, respectively; h_τ is the time stepsize; i, j, k are natural numbers that define the modeling grid. The modeling domain is a 10 × 100 × 100 m prism.

The ground diffusivity at a grid node is

$$a(i,j,k) =$$

$$= \begin{cases} a_\text{f} & \text{at} \quad t(i,j,k,n) < t_f - \Delta, \\ \dfrac{0.5\left(\lambda_\text{f}+\lambda_\text{uf}\right)}{0.5\left(c_\text{f}+c_\text{uf}\right)+L/2\Delta} & \text{at} \quad t_f - \Delta \leq t(i,j,k,n) \leq t_f + \Delta, \\ a_\text{uf} & \text{at} \quad t(i,j,k,n) > t_f + \Delta, \end{cases}$$

where a_f and a_uf are the diffusivities of frozen and unfrozen ground, respectively; λ_f and λ_uf are the thermal conductivities of frozen and unfrozen ground, respectively; c_f, c_uf are the volumetric heat capacities of frozen and unfrozen ground, respectively; L is the latent heat of the phase transition of a soil unit volume; Δ refers to the phase transition temperature range in terms of effective heat capacity.

The evaporator tubes (linear sources of cold) cross the grid nodes. The interaction of the thermosyphon with ground and air is given by [*Spasennikova, 2015*]:

$$U_{i,j,k} = \frac{\lambda_\text{s} h_x h_z}{h_y}\left(t_{i,j+1,k} + t_{i,j-1,k} - 2t_\text{t}\right) +$$

$$+\frac{\lambda_\text{s} h_y h_z}{h_x}\left(t_{i+1,j,k} + t_{i-1,j,k} - 2t_\text{t}\right),$$

$$\sum_{i,j,k\in M} U_{i,j,k} = S_\text{con}\eta_\text{ef}\left(t_\text{t} - t_\text{a}\right)\alpha,$$

where M is the set of grid nodes crossed by a tube; S_con is the surface area of fins on the condenser; η_ef is the efficiency of fins; t_t is the thermosyphon temperature; t_a is the air temperature; λ_s is the thermal conductivite of ground; α is the heat loss from the condenser. The dot product of $\eta_\text{ef}\alpha$ was found by comparing the results of logging and prediction, and the best fit was obtained for $\eta_\text{ef}\alpha = 4.36 + 7.16v$, where v is the wind speed.

The modeling domain has the second- and first-kind boundary conditions on its sides and base (zero heat flow and a temperature equal to the initial temperature, respectively), and a third-kind boundary condition on the top [*Dolgikh et al., 2015*]. Heat exchange across the modeling domain top is assumed to be with the tank beneath the domain and with air in the remaining part.

The climate data are according to records at the Varandey weather station for mean monthly air temperature, wind speed, and snow depth, and to *Building Norms and Regulations* (SP 131.13330.2012) for mean monthly total solar radiation (Table 1).

Heat loss from the finned condenser was calculated for the period between 1 September 2007 and 30 April 2008, on an *NCS-30T* supercomputer at the Siberian Supercomputing Center.

Temperatures were logged in a horizontal (transversal) borehole parallel to the tank bottom (HTB) and in a vertical borehole beneath the tank (IVB) perpendicular to its bottom (Fig. 2). The logging results from the two holes are summarized in Tables 2 and 3, respectively. The respective calculated data are listed in Tables 4 and 5.

Table 1. **Mean monthly air temperatures, wind speed, snow depth, and sun radiation at Varandey weather station**

Date	t_a, °C	v, m/s	h, m	R, W/m²
September 2007	6.7	6.4	0.01	137.5
October 2007	3.1	7.9	0.14	45.7
November 2007	–7.7	6.3	0.21	12.5
December 2007	–7.9	8.1	0.21	–
January 2008	–9.0	8.2	0.45	–
February 2008	–14.7	6.7	0.71	46.1
March 2008	–15.4	7.1	0.79	104.8
April 2008	–9.1	5.7	0.75	219.4

Note. t_a = air temperatures; v = wind speed; h = snow depth; R = solar radiation.

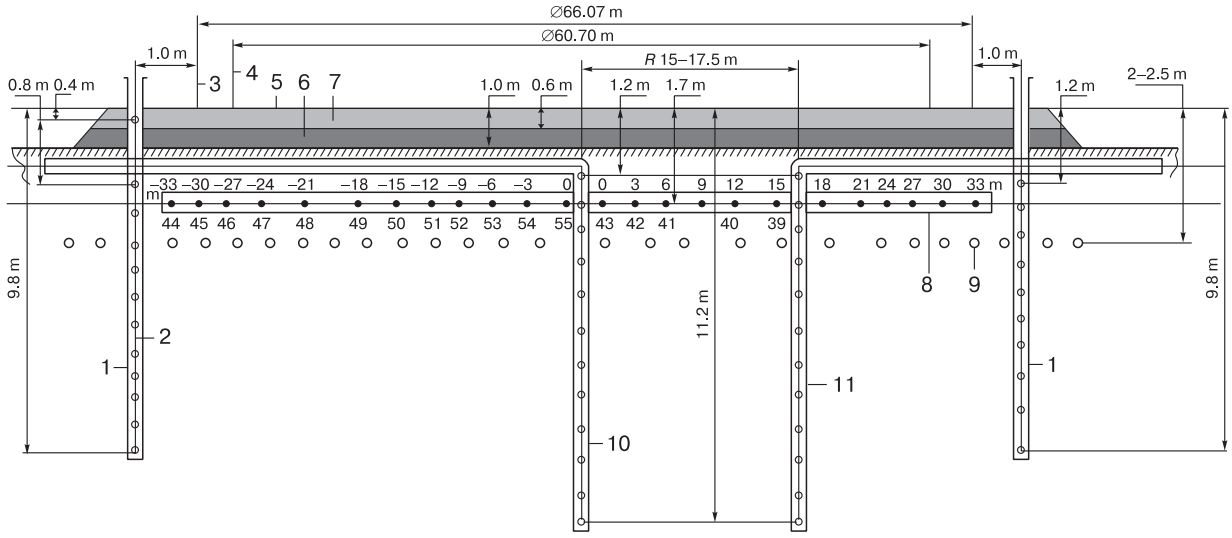

Fig. 2. Location of two boreholes beneath the oil tank.

1 – vertical borehole outside oil tank area (OVB); 2 – cable of thermistors TC-10; 3 – protective wall; 4 – tank wall; 5 – tank bottom; 6 – insulator; 7 – backfill; 8 – horizontal transversal borehole (HTB); 9 – stabilizer of ductile permafrost; 10 – central cable of thermistors in vertical borehole inside oil tank area (IVB); 11 – azimuthal cable of thermistors in vertical borehole inside oil tank.

Table 2. **Measured ground temperatures (°C), HTB**

Date	Distance from center, m											
	Western side											
	–33	–30	–27	–24	–21	–18	–15	–12	–9	–6	–3	0
25.01.2008	–4.52	–5.25	–5.82	–6.22	–5.37	–5.49	–5.14	–5.07	–4.81	–4.54	–5.09	–4.85
05.02.2008	–4.46	–5.01	–5.54	–5.94	–5.16	–5.24	–4.98	–4.90	–4.63	–4.35	–4.86	–4.66
25.02.2008	–7.70	–8.58	–8.77	–9.15	–8.17	–8.74	–7.44	–7.66	–6.71	–6.19	–6.73	–6.59
06.03.2008	–9.35	–9.97	–10.24	–10.77	–9.78	–10.29	–8.92	–9.21	–8.03	–7.50	–8.16	–8.04
16.03.2008	–10.25	–10.78	–11.02	–11.43	–10.43	–10.94	–9.71	–9.99	–8.88	–8.33	–9.07	–8.96
26.03.2008	–9.75	–9.75	–10.31	–10.94	–10.05	–10.19	–9.52	–9.65	–8.79	–8.41	–9.15	–9.00
05.04.2008	–8.25	–8.28	–8.72	–9.04	–8.24	–8.39	–8.16	–8.07	–7.76	–7.45	–8.10	–7.91
18.04.2008	–8.79	–8.51	–8.68	–9.25	–8.38	–8.50	–7.85	–8.03	–7.32	–7.12	–7.73	–7.61
21.04.2008	–8.26	–7.95	–8.14	–8.62	–7.90	–7.88	–7.50	–7.65	–7.00	–6.86	–7.43	–7.26
	Eastern side											
	0	3	6	9	12	15	18	21	24	27	30	33
25.01.2008	–5.21	–5.66	–5.52	–5.58	–5.07	–5.38	–5.78	–6.05	–6.04	–5.79	–3.90	–4.35
05.02.2008	–4.97	–5.36	–5.28	–5.40	–4.99	–5.28	–5.54	–5.76	–5.72	–5.45	–3.72	–4.57
25.02.2008	–7.17	–8.47	–7.88	–8.01	–6.28	–6.56	–8.53	–9.15	–8.89	–9.48	–6.94	–6.00
06.03.2008	–8.59	–9.88	–9.31	–9.34	–7.38	–7.65	–9.79	–10.56	–10.30	–10.80	–8.10	–7.15
16.03.2008	–9.51	–10.78	–10.19	–10.19	–8.18	–8.46	–10.54	–11.31	–11.09	–11.58	–8.91	–9.53
26.03.2008	–9.40	–10.13	–9.92	–9.79	–8.52	–8.76	–9.85	–10.52	–10.40	–10.13	–8.03	–9.08
05.04.2008	–8.26	–8.72	–8.63	–8.58	–7.93	–8.16	–8.55	–8.83	–8.77	–8.43	–6.31	–6.31
18.04.2008	–8.07	–8.68	–8.40	–8.38	–7.50	–7.66	–8.37	–8.82	–8.62	–8.49	–6.72	–8.00
21.04.2008	–7.70	–8.15	–8.00	–7.89	–7.34	–7.52	–7.95	–8.35	–8.18	–7.89	–6.16	–6.78

Table 3. **Measured ground temperatures (°C), IVB**

Date	Depth, m										
	1.2	1.7	2.2	2.7	3.2	4.2	5.2	6.2	7.2	8.2	9.2
25.01.2008	−4.81	−5.02	−4.67	−4.64	−4.15	−3.65	−3.19	−2.63	−2.55	−1.79	−1.22
05.02.2008	−4.62	−4.80	−4.48	−4.50	−4.10	−3.65	−3.24	−2.70	−2.64	−1.86	−1.25
25.02.2008	−6.62	−7.11	−6.67	−5.98	−4.97	−3.95	−3.35	−2.72	−2.65	−1.86	−1.29
06.03.2008	−8.04	−8.35	−7.72	−6.87	−5.74	−4.43	−3.64	−2.89	−2.74	−1.90	−1.30
16.03.2008	−8.92	−9.19	−8.45	−7.52	−6.30	−4.90	−4.00	−3.13	−2.90	−1.96	−1.36
26.03.2008	−8.93	−8.74	−7.90	−7.42	−6.54	−5.26	−4.33	−3.40	−3.09	−2.08	−1.36
05.04.2008	−7.79	−7.82	−7.24	−6.88	−6.16	−5.30	−4.52	−3.62	−3.26	−2.19	−1.44
18.04.2008	−7.66	−7.63	−7.05	−6.99	−6.45	−5.36	−4.55	−3.76	−3.39	−2.37	−1.40
21.04.2008	−7.29	−7.28	−6.76	−6.74	−6.27	−5.34	−4.58	−3.77	−3.42	−2.37	−1.42

Table 4. **Predicted ground temperatures (°C), HTB**

Date	Distance from center, m											
	−33	−30	−27	−24	−21	−18	−15	−12	−9	−6	−3	0
25.01.2008	−1.53	−5.60	−4.94	−4.79	−4.78	−4.78	−4.78	−4.78	−4.78	−4.78	−4.78	−4.78
05.02.2008	−2.30	−6.69	−6.02	−5.87	−5.86	−5.86	−5.86	−5.86	−5.86	−5.86	−5.86	−5.86
25.02.2008	−3.66	−8.84	−8.37	−8.22	−8.22	−8.22	−8.22	−8.22	−8.22	−8.22	−8.22	−8.22
06.03.2008	−4.18	−9.47	−9.04	−8.89	−8.88	−8.88	−8.88	−8.88	−8.88	−8.88	−8.88	−8.88
16.03.2008	−4.70	−10.01	−9.59	−9.44	−9.43	−9.43	−9.43	−9.43	−9.43	−9.43	−9.43	−9.43
26.03.2008	−5.17	−10.37	−9.95	−9.80	−9.80	−9.80	−9.80	−9.80	−9.80	−9.80	−9.80	−9.80
05.04.2008	−5.42	−9.93	−9.55	−9.39	−9.38	−9.38	−9.38	−9.38	−9.38	−9.38	−9.38	−9.38
18.04.2008	−5.43	−8.59	−8.07	−7.84	−7.83	−7.83	−7.83	−7.83	−7.83	−7.83	−7.83	−7.83
21.04.2008	−5.43	−8.35	−7.77	−7.53	−7.52	−7.52	−7.52	−7.52	−7.52	−7.52	−7.52	−7.52
	3	6	9	12	15	18	21	24	27		30	33
25.01.2008	−4.78	−4.78	−4.78	−4.78	−4.78	−4.78	−4.79	−4.94	−4.94		−5.60	−1.53
05.02.2008	−5.86	−5.86	−5.86	−5.86	−5.86	−5.86	−5.87	−6.022	−6.02		−6.69	−2.30
25.02.2008	−8.22	−8.22	−8.22	−8.22	−8.22	−8.22	−8.22	−8.374	−8.37		−8.84	−3.66
06.03.2008	−8.88	−8.88	−8.88	−8.88	−8.88	−8.88	−8.89	−9.037	−9.04		−9.47	−4.18
16.03.2008	−9.43	−9.43	−9.43	−9.43	−9.43	−9.43	−9.44	−9.59	−9.59		−10.01	−4.70
26.03.2008	−9.80	−9.80	−9.80	−9.80	−9.80	−9.80	−9.80	−9.949	−9.95		−10.37	−5.17
05.04.2008	−9.38	−9.38	−9.38	−9.38	−9.38	−9.38	−9.39	−9.552	−9.55		−9.93	−5.42
18.04.2008	−7.83	−7.83	−7.83	−7.83	−7.83	−7.83	−7.84	−8.067	−8.07		−8.59	−5.43
21.04.2008	−7.52	−7.52	−7.52	−7.52	−7.52	−7.52	−7.53	−7.77	−7.77		−8.35	−5.43

Table 5. **Predicted ground temperatures (°C), IVB**

Date	Depth, m										
	1.2	1.7	2.2	2.7	3.2	4.2	5.2	6.2	7.2	8.2	9.2
25.01.2008	−4.78	−5.61	−5.31	−4.68	−4.11	−3.62	−2.87	−2.36	−2.01	−1.78	−1.61
05.02.2008	−5.86	−7.30	−6.37	−5.16	−4.37	−3.82	−3.02	−2.47	−2.09	−1.82	−1.64
25.02.2008	−8.22	−9.22	−8.28	−6.88	−5.69	−4.75	−3.46	−2.71	−2.24	−1.92	−1.69
06.03.2008	−8.88	−9.87	−8.87	−7.42	−6.18	−5.18	−3.74	−2.87	−2.32	−1.97	−1.72
16.03.2008	−9.43	−10.33	−9.38	−7.96	−6.70	−5.64	−4.07	−3.07	−2.44	−2.04	−1.76
26.03.2008	−9.79	−10.64	−9.74	−8.38	−7.13	−6.06	−4.40	−3.29	−2.58	−2.11	−1.80
05.04.2008	−9.38	−9.70	−9.36	−8.51	−7.45	−6.42	−4.71	−3.52	−2.78	−2.20	−1.85
18.04.2008	−7.83	−8.21	−8.17	−7.81	−7.22	−6.50	−5.03	−3.81	−2.93	−2.33	−1.92
21.04.2008	−7.52	−7.93	−7.95	−7.65	−7.13	−6.48	−5.07	−3.87	−2.98	−2.37	−1.94

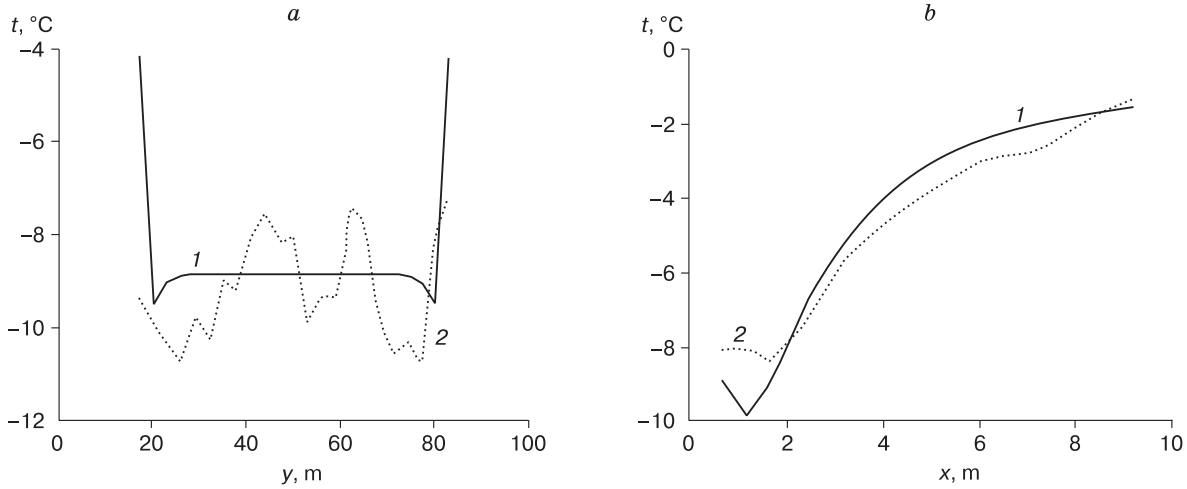

Fig. 3. Predicted (*1*) and measured (*2*) ground temperatures on 06.03.2008.

a: for HTB; *b*: for IVB.

The predicted ground temperatures show good agreement with calculations (Fig. 3).

The accuracy (rms error) of temperature measurements was estimated as

$$\sigma_\Sigma = \sqrt{\sum_i \frac{\left(t_i^t - t_i^e\right)^2}{N-1}},$$

where t_i^t is the calculated temperature at the *i*-th logger; t_i^e is the measured temperature at the *i*-th logger (Tables 2–5); *N* is the total number of loggers used for calculations.

For the segments of the horizontal borehole, where the predicted temperature remains invariable, the rms error is

$$\sigma = \sqrt{\sum_{i\in M} \frac{\left(t_i^t - t_i^e\right)^2}{N-1}},$$

where *M* is the set of loggers within the segment of invariable temperature.

Table 6. **rms error σ, σ_e, σ_Σ for HTB and σ_Σ for IVB on different dates of 2008**

Date	σ	σ_e	σ_Σ, °C	
	°C		HTB	IVB
25.01.2008	0.664	0.409	1.155	0.376
05.02.2008	0.848	0.409	1.216	1.075
25.02.2008	1.421	1.094	1.972	1.044
06.03.2008	1.083	1.083	1.656	0.731
16.03.2008	1.104	1.032	1.656	0.731
26.03.2008	0.726	0.715	1.502	0.971
05.04.2008	1.196	0.409	1.482	1.242
18.04.2008	0.623	1.083	1.114	0.679
21.04.2008	0.491	0.460	0.910	0.720

It is also interesting to estimate the rms error of experimentally measured temperatures (σ_e):

$$\sigma_e = \sqrt{\sum_{i\in M} \frac{\left(\overline{t}^e - t_i^e\right)^2}{N-1}}, \quad \overline{t}^e = \sum_i \frac{t_i^e}{N}.$$

The calculations are of high accuracy: the rms errors are mostly within 1 °C for the vertical borehole and for the segment of invariable temperature in the horizontal borehole though 1.5 °C within the segments of temperature variations (see summed σ_Σ, σ_e and σ values for different dates in Table 6).

Probabilistic analysis of temperatures

The state of ground at different scenarios of climate change and the probability for finding unfrozen soil at arbitrary points were estimated using probabilistic prediction with the stochastic analysis. The probabilities for air temperature and wind speed were evaluated for each month with reference to data from the Varandey weather station (Table 7). The derivation was detailed by *Dolgikh et al.* [*2015*].

The probability for air temperatures fits the lognormal distribution [*Melnikov et al., 2014*]:

$$w(t) = \frac{\exp\left(-\left(t-\overline{t}\right)^2 / 2\sigma^2\right)dt}{\sqrt{2\pi}\sigma},$$

where *t* is the air temperature, °C; $\overline{t}$ is its mathematical expectation; $\sigma = \sqrt{D_t}$ is its rms deviation; D_t is its variance.

The probability for wind speed fits quite well the gamma law [*Melnikov et al., 2014*]:

$$w(v) = \frac{\lambda^{\beta_v}}{\Gamma\left(\beta_v\right)} v^{\beta_{v-1}} \exp\left(-\lambda_v v\right)dv,$$

Table 7. **Parameters of distribution for each month**

Parameter	January	February	March	April	May	June	July	August	September	October	November	December
$\bar{t}$, °C	−14.78	−18.9	−13.0	−7.13	−1.55	6.07	10.72	9.16	6.47	1.53	−7.83	−11.03
σ, °C	7.18	8.8	6.93	6.61	5.09	5.9	4.6	3.0	3.16	3.49	7.7	9.02
β_v	3.04	3.07	2.73	3.79	4.0	3.57	3.86	4.94	3.4	5.03	2.73	4.73
λ_v	0.47	0.48	0.48	0.67	0.72	0.67	0.66	0.82	0.6	0.74	0.52	0.62

Table 8. **Variations along x aixs (x_j) and probability (Wc_j) for finding unfrozen soil along IVB line**

j	x_j, m	Wc_j, %
0	0.7	3.9
1	1.2	1.2
2	1.7	0.44
3	2.2	0.16
4	2.7	0.06
5	3.2	0.02
6	4.2	0.002
7	5.2	0
8	6.2	0
9	7.2	0
10	8.2	0
11	9.2	0

Note: for latest August of eighth year.

Table 9. **Variations along y aixs (y_i) and probability (Wm_i) for finding unfrozen soil along HTB line**

i	y_i, m	Wm_i, %	i	y_i, m	Wm_i, %
0	17	98.8	12	53	4.2
1	20	0.27	13	56	4.2
2	23	3.1	14	59	4.2
3	26	3.9	15	62	4.2
4	29	4.1	16	65	4.2
5	32	4.1	17	68	4.1
6	35	4.2	18	71	4.1
7	38	4.2	19	74	3.9
8	41	4.2	20	77	3.1
9	44	4.2	21	80	0.27
10	47	4.2	22	83	98.8
11	50	4.2			

Note: for latest August of eighth year.

where v is the wind speed; $\Gamma(\beta_v)$ is the gamma function, β_v and λ_v are related with the mathematical expectations for the wind speed $\bar{v}$ and its variance D_v as:

$$\bar{v} = \frac{\beta_v}{\lambda_v},\ D_v = \frac{\beta_v}{\lambda_v^2},\ \lambda_v = \frac{\bar{v}}{D_v},\ \beta_v = \frac{\bar{v}^2}{D_v}.$$

The generation of 47 × 8 air temperature and wind speed values using a *Mathcad-14* random number generator (Table 7) yields 47 eight years-long scenarios of time-dependent changes in these parameters. The 3D temperature field of latest August is obtained by calculations for a period from September 1 to August 31 of the eighth year for each scenario.

The snow depth and solar radiation are assumed to be the same through all months. With these data, temperature values were calculated along a line coin-

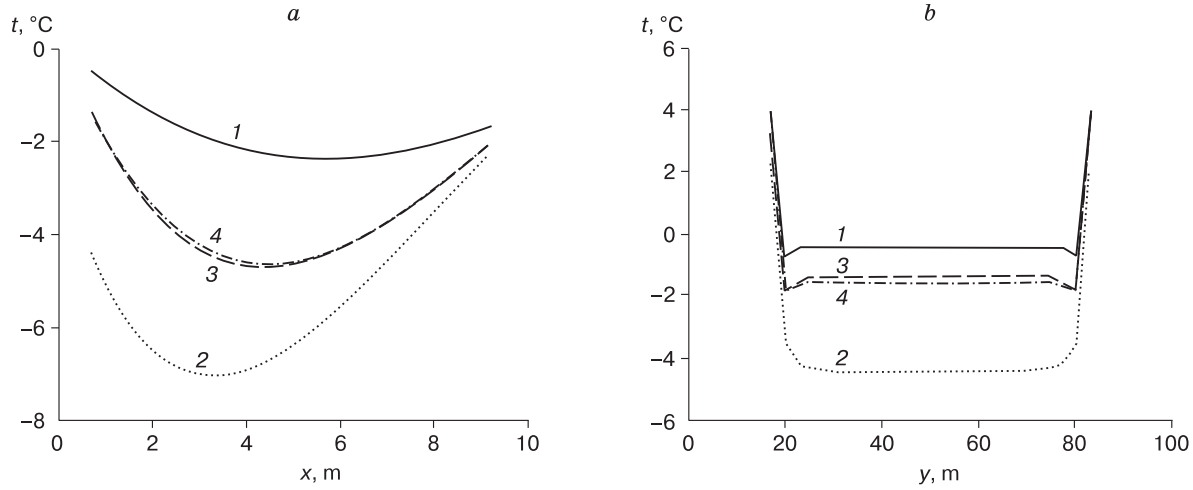

Fig. 4. Ground temperature variations on latest August of the eighth year of calculations.

a: IVB line; *b*: HTB line; *1* – warmest scenario; *2* – coldest scenario; *3* – closest to arithmetic mean over all considered scenarios; *4* – arithmetic mean over all considered scenarios.

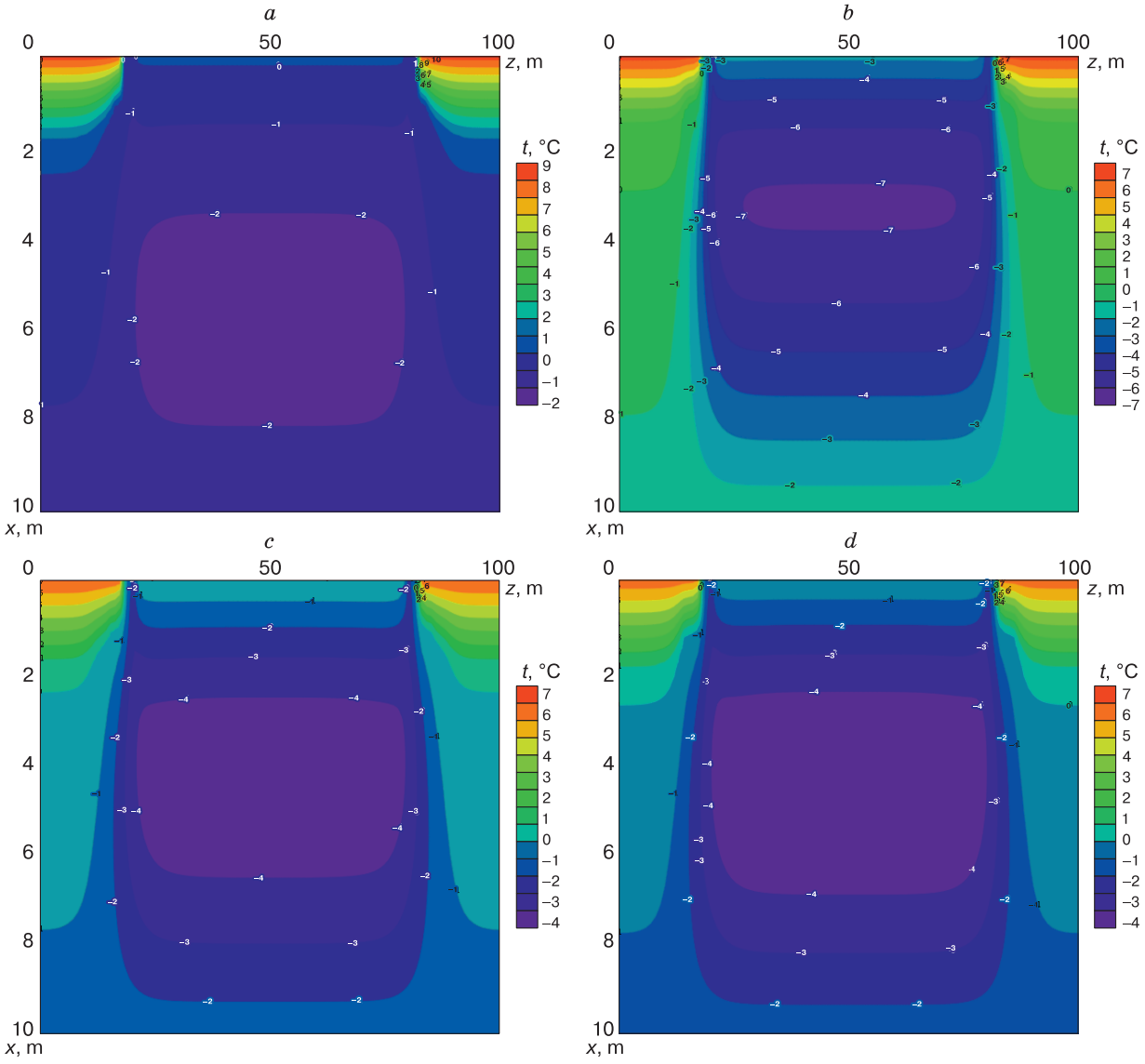

Fig. 5. Temperature field on latest August of the eighth year of calculations, for scenarios in the y = 50 m plane that crosses the tank center parallel to the evaporator tubes.

a: warmest scenario; *b*: coldest scenario; *c*: closest to average over random trajectories along IVB line; *d*: closest to average over random trajectories along HTB line.

ciding with the IVB axis from the obtained forty seven 3D temperature fields for latest August of the eighth modeling year, at the locations of temperature loggers: $x = x_j$ ($0 \leqslant j \leqslant 11$), y = 50 m, z = 50 m (see Table 8 for x_j values).

In the same way, temperatures were calculated along a line coinciding with HTB at the locations of the loggers: x = 0.7 m, $y = y_i$ ($0 \leqslant i \leqslant 22$), z = 50 m (see Table 9 for y_i values).

The probability of finding unfrozen soil along the lines IVB and HTB in the end of August of the eighth year was estimated assuming lognormal distribution of ground temperatures. With this assumption, the probability for >0 °C temperatures to occur at the j-th point along the IVB line is

$$Wc_j = 100\,\% \cdot \int_0^{\infty} \frac{\exp\left(-\left(t-\overline{tc}_j\right)^2 \Big/ 2\overline{\sigma c}_j^2\right)}{\overline{\sigma c}_j\sqrt{2\pi}} dt, \quad (1)$$

where $\overline{tc}_j$ is the mathematical expectation for ground temperature at the j-th point along the IVB line and $\overline{\sigma c}_j$ is the rms error of this temperature.

The probability for the temperature >0 °C to occur along the HTB line is

$$Wm_i = 100\,\% \cdot \int_0^{\infty} \frac{\exp\left(-\left(t-\overline{tm}_i\right)^2 \Big/ 2\overline{\sigma m}_i^2\right)}{\overline{\sigma m}_i\sqrt{2\pi}} dt, \quad (2)$$

where $\overline{tm}_i$ is the mathematical expectation for ground temperature at the i-th point along HTB; $\overline{\sigma m}_i$ is the rms error of this temperature. Both probabilities are in percent.

The calculations confirm the reliability of the refrigeration system: according to the Wc_j (Table 8) and Wm_i (Table 9) values found with equations (1) and (2), unfrozen soil may occur at the depth 0.7 m below the insulator layer, along HTB, to a probability of ~4 %.

Figure 4 shows the variations of ground temperature along IVB on the x axis for the coldest and warmest scenarios; the arithmetic mean over all considered scenarios; and the scenario which is the closest to the arithmetic mean (*a*) and the respective parameters for the line HTB along the y axis (*b*).

Note that the scenario closest to the temperature averaged over all scenarios is the Stefan solution, while the temperature itself is not. As follows from Fig. 4, this scenario can be considered as average over the statistical sample of random trajectories.

The temperature fields in the plane y = 50 m are shown in Fig. 5 for each scenario.

CONCLUSIONS

The reported comparison of probabilistic predictions with temperature logging data has demonstrated good agreement, i.e., the prediction method we suggested [*Anikin et al., 2011a, 2013; Dolgikh et al., 2013, 2014, 2015; Melnikov et al., 2014*] is applicable to stochastic analysis.

The refrigeration system beneath the oil tank at the Varandey oil field ensures reliable thermal stabilization of permafrost: the probability of finding unfrozen soil beneath the tank is within 4.2 %.

The study was carried out as part of Basic Research Program of the Russian Academy of Sciences (Project IX.135.2.4). Data processing on the NCS-30T supercomputer at the Siberian Supercomputing Center was supported by grant 18-38-00068 mol_a from the Russian Foundation for Basic Research.

References

Anikin, G.V., Plotnikov, S.N., Vakulin, A.A., Spasennikova, K.A., 2009. Modeling of temperature stabilization beneath an oil tank. Bull. Tyumen Univ., No. 6, 35–45.

Anikin, G.V., Plotnikov, S.N., Spasennikova, K.A., 2011a. Computer simulation of heat-mass exchange in the systems of horizontal ground cooling. Kriosfera Zemli XV (1), 33–39.

Anikin, G.V., Plotnikov, S.N., Spasennikova, K.A., 2011b. Stationary temperature fields in the system "oil tank – thermosyphon". Kriosfera Zemli XV (2), 29–33.

Anikin, G.V., Plotnikov, S.N., Vakulin, A.A., Spasennikova, K.A., 2013. Probabilistic prediction of soil behavior under structures built on permafrost. Bull. Tyumen University, No. 7, 46–53.

Anikin, G.V., Spasennikova, K.A., 2012. Computer modelling of the ground cooling system under the oil-tank. Kriosfera Zemli XVI (2), 60–64.

Anikin, G.V., Spasennikova, K.A., 2013. Software *Stohastic – 3D*. Certificate of State Registration No. 2013612566. FIPS, 1 p.

Anikin, G.V., Spasennikova, K.A., Ishkov, A.A., Plotnikov, S.N., 2017a. Operation of a thermosyphon with a horizontal evaporator tube: updated probabilistic prediction. Osnovaniya, Fundamenty i Mekhanika Gruntov, No. 6, 30–34.

Anikin, G.V., Spasennikova, K.A., Plotnikov, S.N., Ishkov, A.A., 2017b. Probabilistic prediction of soil temperature stabilized with a HET thermosyphon system. Osnovaniya, Fundamenty i Mekhanika Gruntov, No. 1, 35–40.

Building Norms and Regulations, 2012. Working Document SP 131.13330.2012. Construction Climatology. Actual Edition SNiP 23-01-99*. Minregionrazvitiya RF, Moscow, 109 pp.

Dolgikh, G.M., Anikin, G.V., Rilo, I.P., Spasennikova, K.A., 2015. Statistical modelling of "GET" system installed at the base of oil reservoir. Earth's Cryosphere (Kriosfera Zemli) XIX (1), 61–68.

Dolgikh, G.M., Okunev, S.N., Anikin, G.V., Spasennikova, K.A., 2013. Simulation of non-stationary temperature fields in the system "oil tank – thermosyphon". Kriosfera Zemli XVII (3), 70–75.

Dolgikh, G.M., Okunev, S.N., Anikin, G.V., Spasennikova, K.A., Zalesskiy, K.V., 2014. Comparison of experimental and numerical modelling data of the work of "GET" cooling system on the example of fire depot of the Vankorsky field. Earth's Cryosphere (Kriosfera Zemli) XVIII (1), 65–69.

Melnikov, V.P., Melnikova, A.A., Anikin, G.V., Ivanov, K.S., Spasennikova, K.A., 2014. Building on permafrost: engineering solutions for energy efficiency. Earth's Cryosphere (Kriosfera Zemli) XVIII (3), 76–82.

Plotnikov, S.N., Anikin, G.V., Melnikov, V.P., Rusakov, N.L., 2017. Software *Arctica 3D MPI*. Certificate of State Registration No. 2017618746. FIPS, 1 p.

Spasennikova, K.A., 2015. Simulation of Heat and Mass Transfer in Soils under Structures on Permafrost Stabilized by Thermosyphons. Author's Abstract, Candidate Thesis (Engineering). Tyumen, 19 pp. (in Russian)

Received May 10, 2018
Revised version received August 27, 2018
Accepted September 24, 2018